THE INFLUENCE OF SURFACE FEATURES ON BACTERIAL COLONIZATION AND SUBSEQUENT SUBSTRATUM CHEMICAL CHANGES OF 316L STAINLESS STEEL

G. G. GEESEY,[1] R. J. GILLIS,[1] R. AVCI,[2] D. DALY,[3] M. HAMILTON,[3] P. SHOPE[4] and G. HARKIN[4]

[1] Department of Microbiology, [2] Department of Physics, [3] Department of Mathematical Sciences,
[4] Department of Computer Science, Center for Biofilm Engineering, Montana State University, Bozeman, MT 59717, U.S.A.

Abstract—Biofilm-forming bacteria were found to selectively colonize specific surface features of unpolished 316L stainless steel exposed to flowing aqueous media. Depending on the types of bacteria present, selective colonization resulted in significant depletion of Cr and Fe relative to Ni in the surface film at these features. No such depletion was observed on uncolonized surfaces exposed to sterile flowing aqueous medium. The results demonstrate that non-random, initial colonization of 316L stainless steel surfaces by these bacteria leads to changes in alloy elemental composition in the surface film that are enhanced with time. These chemical changes may be a critical step that weakens the oxide film at specific locations, allowing halides such as Cl^- ions greater access to the underlying bulk alloy, and thereby facilitates localized attack and pit formation and propagation.

Keywords: A. stainless steel, C. microbiological corrosion, C. pitting corrosion.

INTRODUCTION

The involvement of micro-organisms in localized attack of stainless steels (SS) has been proposed by a number of investigators.[1–6] Although the mechanisms of microbially influenced corrosion (MIC) are largely based on speculation at the present, progress has been made on identification of metallurgical features associated with MIC.[7,8] In the case of stainless steels, weld and heat-affected zones are most susceptible to MIC-associated pitting corrosion.[9,10] Base metal attack is less common, although it has been observed. The majority of chemical evidence attributing certain types of localized corrosion to micro-organisms on metal surfaces has been based on data obtained from surface deposits which have accumulated long after the corrosion reaction was initiated.[11] Unfortunately, the chemistry of the deposits does not necessarily offer insight to the critical, initial microbially-mediated reactions that compromise the protective surface oxide film in the presence of a developing biofilm.

Segregation of elements occurs between grains of alloys such as stainless steels.[9,12] Chromium, which is the alloying element that makes steel stainless, can be depleted in these regions when the alloy has been sensitized and lead to preferential anodic dissolution in these alloys.[12,13] Little *et al.*[14] presented evidence for microbially-assisted depletion of nickel in 90/10 and 70/30 copper–nickel in seawater. In this paper we describe the conditions under

which surface-associated microbes promote selective depletion of elements such as chromium at grain boundaries of the surface oxide film on unpolished 316L stainless steel.

Detection of near-surface chemical changes mediated by film-forming bacteria requires surface sensitive analytical techniques. X-ray photo-electron spectrometry (XPS) and Auger electron spectrometry (AES) provide information on the elemental composition and chemistry of the top 1–6 nm of the metal surface. Bruemmer[12] used AES to characterize grain boundary composition. To date, these types of analyses have only been included in a few MIC studies.[15] To our knowledge, no studies on chemical changes in the surface oxide film during early stages of microbial surface colonization have been conducted with stainless steels. Subtle changes in surface chemistry at this stage of biofilm development should help clarify the role of biofilm microbes in localized pitting corrosion of stainless steels.

The colonization and growth of bacteria on a metal surface results in a biofilm which displays non-uniform coverage over the surface.[16]. Until recently, little was known about what controls the colonization of bacteria on metal surfaces in contact with flowing fluids. Mueller *et al.*[17] reported that attachment of cells of *Pseudomonas aeruginosa* and *Pseudomonas fluorescens* to hand polished 316 SS in a laminar flow fluid field was positively correlated with surface free energy, surface roughness and hydrophobicity. Walsh *et al.*[11] concluded, on the basis of microscopic observations, that initial bacterial attachment was random and that bacterial proliferation, biofilm development and consortia formation was determined by metallurgical features that promote the production of high concentrations of microbial metabolites.

In some cases, intergranular attack and pitting are believed to be associated with the presence of bacteria.[18] Walsh *et al.*[11] concluded that pits formed at locations adjacent to bacterial accumulations on surfaces and only in rare cases was pitting observed directly beneath a biofilm at early stages of growth. Similar observations were made with respect to the locations of pits and accumulations of biofilm bacteria on fully hydrated copper coupons using atomic force microscopy.[19] Preferential corrosion attack is not uncommon at grain boundaries, triple points and large inclusions adjacent to microcolonies of bacteria.[11]

In this paper the selective colonization of surface features of unpolished 316L SS by defined pure and mixed cultures of biofilm-forming bacteria are described together with the changes in the elemental composition at these surface features that accompany the colonization process. A rigorous quantitative and statistical approach has been used to verify the relationships between surface features, surface film chemistry and microbial colonization. Based on these results, a mechanism is proposed for the role of biofilm micro-organisms in the localized attack of unpolished forms of this alloy.

EXPERIMENTAL

Coupon preparation

Unpolished, mill-run coupons (20 × 2 cm) made of 20 gauge (0.9144 mm) 316L stainless steel with a 2B finish (as received) were obtained from Metal Goods Services, Spokane, WA. The as-received coupons were cut from a coil of product that had been hot rolled (2300°F), pickled and passivated, cold-rolled, solution annealed at 2050°F, rapidly cooled and subjected to a final cold role to flatten and shape. The as-received product exhibited an ASTM #7 grain size. The 2B finish that was applied to the product was based on the procedure described by Lula.[20] As-received coupons to be used in reactors for microbiological studies were cleaned and repassivated according to ASTM Standard

Practice A-380-78 code F.[21] Passivation involved treatment with 50% nitric acid at 71°C for 30 min. A polishing step was not included in this study in order to simulate surface conditions of material that is placed in service without this treatment.

For bulk grain structure analysis, as-received coupons were mounted in phenol–formaldehyde medium, subjected to wet grinding on silicon carbide papers, 120–600 grits, then polished with 12 and 3 μm diamond lap. The polished coupons were etched in 60/40 HNO_3/H_2O for 45 s according to standard procedures.[22] After etching, photographs of the surface were taken using a camera mounted on a metallographic microscope. Grain area was estimated by cutting out images of 134 individual grains on photographic paper, weighing the paper and comparing with the weight of paper representing standardized areas.

Bacteria

The facultative anaerobic bacterium, *Citrobacter freundii*, and the sulfate reducing bacterium, *Desulfovibrio gigas*, were used in these studies. *C. freundii*, identified by an Analytical Profile Index (API) 20E assay (Analytical Products Division, Sherwood Medical, Plainview, NY), was an environmental isolate from an active tubercle from a Tennessee Valley Authority pipeline obtained from M.W. Mittelman, University of Tennessee at Knoxville. *D. gigas* (ATCC #19364) was obtained from the American Type Culture Collection (ATCC) Rockville, MD. It was selected for the study because this species of sulfate reducing bacterium had also been isolated from the corroding stainless steel pipeline. Its large cell size (5 × 40–50 μm) and spirilloid shape permitted differentiation from *C. freundii* (short rod) by microscopic examination in coupon colonization and suspended culture studies.

Culture medium

The culture medium (EPRI) used for the flow-through reactor studies is described in Tables 1–3. The medium was steam sterilized for 15 min at 121°C, then incubated at 22°C for 7 days to assure sterility. If no turbidity (indicating microbial contamination) was observed in the medium after 7 days, it was diluted 1:10 in de-ionized (DI) water in a carboy, sterilized by autoclaving and amended with filter sterilized solutions of 10 ml sodium sulfite (0.13 g ml^{-1}), 3.3 ml of 10 mM ferric chloride and 10 ml of modified Hutner's salts solution.[23] The final pH of the culture medium was 7.2. The total organic carbon content of the culture medium was approximately 45 ppm.

Table 1. Composition of EPRI medium for culturing bacteria in flow-through reactor

Sodium lactate	500 mg
Sodium succinate	500 mg
Ammonium nitrate	500 mg
Sodium sulfate	500 mg
Yeast extract	500 mg
Monobasic potassium phosphate	1.9 g
Dibasic potassium phosphate	6.3 g
Modified Hutner's salts solution	10 ml

Quantities specified per 1 liter deionized water.

Table 2. Composition of Hutner's salt solution

Nitrilotriacetic acid	10 g
$MgSO_4$	14.45g
$CaCl_2. 2H_2O$	3.335g
$(NH_4)_6Mo_7O_{24} 4H_2O$	9.25 mg
$FeSO_4 H_2O$	99.0 mg
Metals '44' solution	50 ml

Quantities specified per 1 liter deionized water.

Table 3.   Metals '44' solution

Ethylenediaminetetraacetic acid	250 mg
$ZnSO_4 7H_2O$	1095 mg
$FeSO_4 7H_2O$	500 mg
$MnSO_4 H_2O$	154 mg
$CuSO_4 5H_2O$	39.2 mg
$Co(NO_2)_2 6H_2O$	24.8 mg
$Na_2B_4O_7 10H_2O$	17.7 mg

Quantities specified per 100 ml.

Reactor preparation and inoculation

The reactor consisted of several silicone tubes, each containing a stainless steel coupon, through which sterile culture medium, diluted 1:10 with DI water, was fed by a peristaltic pump from a common reservoir (Fig. 1). The reactor was assembled, connected to the reservoir containing DI water and leak-tested before adding the EPRI medium to the reservoir and steam sterilizing the entire system for 15 min at 121°C.

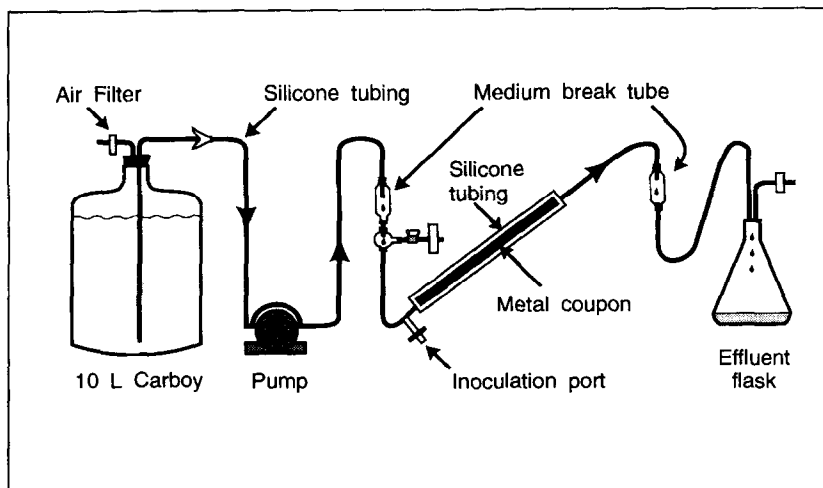After sterilization, the reactor was placed in an anaerobic chamber. Sterile anaerobic

Fig. 1.   Schematic diagram of flow-through anaerobic reactor used to establish microbial biofilms on surfaces of 316L SS coupons.

EPRI medium, diluted 1:10 with sterile DI water, was pumped from the reservoir through each set of silicone tubing. The flow rate of the medium through each set of tubing was 1.6×10^{-3} cm s^{-1}. This flow rate was selected to mimic flow conditions where corrosion problems in stainless steel piping systems have been observed (Susan Borenstein, Structural Integrity Associates, Inc., San Jose, CA; personal communication). The volume of each set of silicone tubing was approximately 60 ml, providing a culture medium residence time of approximately 3 h. The effluent from each set of tubing was sampled and tested for contamination by the AODC method before inoculation of selected tubing.

Each silicone tube containing an SS coupon was inoculated with a different combination of bacteria (*D. gigas* only; *C. freundii* only; *D. gigas* and *C. freundii* together), except for one in each experiment which was maintained as a sterile control. The tube inoculated with *C. freundii* received a one time inoculum of 1×10^7 cells, as verified by AODC and enumeration of colony forming units (CFU) after plating on MacConkey Agar as described below. The *C. freundii* inoculum was obtained from a 24 h anaerobic batch culture in EPRI medium maintained at 22°C. The tube inoculated with only *D. gigas* received an initial inoculum of 1×10^5 cells, as verified by AODC. The inoculum was obtained from a 14-day anaerobic culture in EPRI medium maintained at 22°C. The tube receiving inocula of both types of bacteria was inoculated with a similar number of cells of each species as described above. The inoculum of *D. gigas* was introduced after the concentration of *C. freundii* in the reactor effluent (derived from the biofilm growing on the coupon and reactor surface) had achieved a steady level. The concentration of *D. gigas* in the reactor effluent was determined daily by AODC while the concentrations of *C. freundii* were determined by AODC and plating on MacConkey's Agar until the experiment was terminated, at which time the coupons were recovered for microbiological and surface chemical characterization.

Coupon sampling

At the termination of the flow-through reactor experiments, each silicone tube was cut open using a sterile razor blade, the culture media poured into a sterile beaker, and the coupon removed with sterile forceps. Each coupon was quartered into 2×5 cm sections using sterile tin snips. Three sections were placed directly into liquid nitrogen for subsequent analysis by Auger electron spectroscopy (AES), while the remaining section was prepared for enumeration of attached bacteria using the following procedure. The bacteria were scraped off one side of the section of coupon with a sterile scalpel blade and transferred to a vial containing sterile phosphate buffer (PB; 0.19 g l^{-1} KH$_2$PO$_4$ and 0.63 g l^{-1} K$_2$HPO$_4$). The cell suspension was vortexed to disperse the cells, diluted with PB and *C. freundii* enumerated by AODC and by plating on MacConkey Agar while *D. gigas* was enumerated by AODC and the three-tube Most Probable Number (MPN) method as described below.

Enumeration of bacteria

CFU and AODC were used to determine concentrations of *C. freundii* in reactor effluents. For enumeration using the culture method, effluents were serially diluted in PB, plated on MacConkey Agar and incubated at 22°C for 24 h under aerobic conditions before enumerating colony forming units (CFU). Preliminary studies indicated that no significant difference in recoverable CFU was detected when anaerobically-grown cells of *C. freundii* were incubated on MacConkey Agar under aerobic or anaerobic conditions. The three-tube Most Probable Number (MPN) was carried out in anaerobic EPRI medium to enumerate

D. gigas.[24] MPN tubes were considered positive for the SRB if they contained black iron sulfide precipitate after incubation at 25°C for 2 weeks.

Densities of *C. freundii* and *D. gigas* in tubing effluents were determined by AODC using conventional epifluorescence microscopy. Aqueous suspensions of bacterial cells ranging in volume from 0.1 to 1.0 ml were mixed with 0.1 ml of a 1 μg ml^{-1} aqueous solution of acridine orange and the final volume adjusted to 2 ml by addition of PB. After a 5 min staining period, the cell suspensions were filtered through blackened polycarbonate membranes (25 mm dia., 0.22 μm pore size) mounted on glass filtration assemblies. The membrane containing the trapped cells was transferred to a glass microscope slide, a drop of immersion oil applied to the membrane surface and a coverslip applied before examining with an Olympus BH2 microscope (Olympus Optical Co. Ltd., Japan) equipped with an ocular counting grid and an Olympus BH2-RFL-T2 mercury lamp. An Olympus BP490 filter (excitation 490 nm, barrier 515 nm) was used for viewing acridine orange stained preparations. Cells of *C. freundii* were enumerated at 1000 × magnification, while cells of *D. gigas* were enumerated at 400 × and distinguished from *C. freundii* on the basis of size. Bacterial densities were based on counts from at least 30 fields.

A segment of each coupon over which the biofilm had not been disturbed was submerged for 5 min in a sterile 1μg ml^{-1} aqueous solution of the fluorochrome, 4,6 diamidino-2-phenylindole (DAPI), rinsed with PB, air dried and then viewed under the Olympus microscope described above using a UG1 filter combination (excitation 340 nm, barrier filter 420 nm) to determine sterility of the coupon in the uninoculated silicone tube as well as cell densities of *D. gigas* attached to the undisturbed coupon surface. Cells displaying the size characteristic of *D. gigas* in at least 30 fields were counted and used to estimate their density on the coupon surface.

Coupon segments used for determining surface-associated bacterial distribution and density evaluation by confocal scanning laser microscopy (CSLM) were prepared in a manner similar to that described above except that a 1 μg ml^{-1} aqueous solution of acridine orange was substituted for DAPI because the laser energy was outside the excitation range for the latter fluorochrome. CSLM images of segments of the coupon surface were collected using a Bio-Rad® Model MRC-600 confocal scanning laser microscope equipped with a krypton/argon laser (Bio-Rad Microscience Division, Cambridge, MA) using a 488 nm excitation and 505 nm barrier filter. The CSLM was used in conjunction with an Olympus microscope (Model BH2, Olympus Optical Co. Ltd., Japan) equipped with an Olympus D Plan Apo UV series 160/1.30 oil immersion objective. Ten randomly chosen fields were examined per coupon segment at 2000 × magnification. For each field, two images were saved as digitized images (pic files) using the Bio-Rad® Comos software. One image was a reflected white light image of the stainless steel surface, showing surface features of the alloy. The second image was an epifluorescent image of acridine orange-stained, surface-associated bacteria.

Image processing and analysis

Quantitative summaries of the images were computed using in-house software called MARK. Details of the procedure are presented in the Appendix.

Energy dispersive analysis by X-rays

Sections of coupons as-received from the supplier as well as sections recovered after cleaning and repassivation were evaluated by energy dispersive X-ray analysis/scanning

electron microscopy (EDX/SEM) to verify bulk elemental abundances reported by the coupon manufacturer. Coupons were examined using a JEOL model JSM 6100 scanning electron microscope equipped with an energy dispersive X-ray spectrometer and software (Noran Instruments, Middleton, WI) using a 15 kV electron beam. Under these operating conditions, the electron beam penetrated approximately 0.85 μm into the stainless steel based on a material density of 8.03g /cm^{-3}.[25] The elements were quantified from each spectrum using standardless analysis routine on Norton software. Spectral data were also gathered from areas corresponding to grains and grain boundaries of the surface oxide film on each coupon. The beam was focused on the feature of interest to allow elemental data to be acquired from each feature independently utilizing point spectroscopy.

Auger electron spectroscopy

A scanning Auger electron spectrometer (Perkin-Elmer, Physical Electronics Division, Phi Model 595, Eden Prairie, MN) equipped with a scanning Auger microprobe (Physical Electronics Instruments Inc., Eden Prairie, MN) coupled to a computer interface was used to obtain surface elemental information on segments of the as-received coupons as well as segments of coupons recovered at the end of an experiment. Surfaces were sputtered using an argon ion beam to penetrate the region that was heavily contaminated by carbon contributed by the aqueous medium and/or the biofilm. Four sequential sputtering events of 15 s intervals (0.5 μA current, 3 keV beam rastered within a 3 $\times$ 3 mm^2 area) were carried out, each followed by a survey Auger analysis of three fields at 2000 $\times$ magnification, each covering an area of approximately 50 $\times$ 50 μm to locate the region below the surface of the film where carbon contamination was reduced to a level where this element contributed approximately 10% of the total elemental abundance. Using a sputtering rate of 0.1 nm s^{-1}, based on pure silicon dioxide, we determined the region where the carbon abundance was reduced to this level to be approximately 6 nm below the surface. Small spot Auger spectroscopic analysis was then employed to gather spectra from three fields (0.79 μm^2) within a grain or grain boundary of the oxide film within the sputtered area. The vacuum chamber of the spectrometer was baked out prior to sample introduction in order to eliminate the possibility of chamber-derived carbon contamination of the sample.

Relative elemental percentages were calculated for each spectrum by measuring the peak height (PH_i) of each respective element (E_i), dividing by a known sensitivity factor (SF_i) for that element, then normalizing to 100% as shown in equation (1) as described by Davis et al.[26]

$$\text{Rel. elemental \% for } E_i = \frac{\frac{PH_i}{SF_i}}{\sum_{j=1}^{I} \frac{PH_j}{SF_j}} \times 100 \text{ \%}, \tag{1}$$

where I = number of elements of interest, $i = 1, 2, ..., I$.

The elemental percentage from each of the following elements was calculated: silicon, phosphorus, sulfur, chlorine, potassium, carbon, nitrogen, oxygen, chromium, iron, nickel and sodium. Auger electron kinetic energies (KE) were used to determine peak locations on each spectrum for each element and the sensitivity factors (SF) were used to calculate elemental percentages as shown in Table 4. Data on molybdenum, one of the key alloying elements in 316L SS, was not included in this survey because the peak for calibrating this element at 2044 eV is outside the energy window used to analyse the other elements of interest. The lines at 186 and 221 eV were too weak to obtain useful data.

Table 4.   Kinetic energies (KE) and sensitivity factors (SF) used for elemental percentage calculations

	Si	P	S	Cl	K	C	N	O	Cr	Fe	Ni	Na
KE	82	130	153	180	235	252	380	505	525	605	750	980
SF	0.35	0.52	0.80	1.0	0.80	0.20	0.30	0.50	0.35	0.20	0.27	0.22

Chromium to nickel and iron to nickel ratios were calculated for each spectrum collected after the fourth 15 s sputtering interval (60 s total sputtering time) in order to obtain alloy elemental abundances below the carbon contaminated surface layer of the oxide film. Although the presence of carbon should not affect the abundance of the alloying metals (Cr, Fe and Ni) with respect to each other, excessive carbon contamination (> 25% carbon elemental abundance) does reduce the contribution of the alloying elements to levels that compromise the accuracy of the resulting ratios. The region sampled below the layer that is heavily contaminated with carbon will be referred to as the near surface.

Atomic force microscopy

Atomic force microscopy (AFM) was performed on as-received coupons and repassivated coupons exposed to bacteria to determine the topography of the oxide film. The coupons were imaged in air using a Nanoscope III multimode AFM (Digital Instruments, Santa Barbara, CA). The AFM was equipped with a 450 μm silicon cantilever (Digital Instruments) with an imaging force of approximately 10^{-8} N. Three different AFM sections were analysed in three different areas of each coupon. The average vertical displacement across a grain boundary in the surface oxide film was determined from 24 measurements beginning at the top of one grain and ending at the lowest point in an adjacent grain boundary. An average width of a grain boundary was determined from 12 horizontal distance measurements from the edge of one grain to the edge of another adjacent grain in the oxide film.

Statistical analyses

Statistical significance tests were conducted to see if the data contradict the null hypothesis that bacteria have no preference for attachment to grains over grain boundaries in the surface oxide film. According to the null hypothesis, the probability of a bacterium attaching in a region (grain or grain boundary) equals the proportion of the area of interest represented by that region. The test statistic, denoted by C, is defined in eqn (2).

$$C = \sum_{i=1}^{n} \frac{N_i(Q_i - P_i)_2}{P_i(1 - P_i)}, \text{ where} \tag{2}$$

Q_i = percentage of bacteria within area of interest that are within a grain boundary, P_i = percentage of area of interest containing grain boundaries, N_i = total bacteria within area of interest, i = image number, and n = number of images.

If the null hypothesis were true, the statistic C follows a chi-squared probability distribution with n degrees of freedom. By reference to that distribution, the p-value was found. The p-value is the chance of a C as large as observed if the null hypothesis were true.

For each AES measurement (raw elemental percentage, ratio, and adjusted percentage), the null hypothesis that the true mean for grains equals the true mean for grain boundaries

was tested using a two-tailed, unpaired *t*-test. The test statistics and associated *p*-values were calculated using the InStat computer program (version 1. 13, GraphPAD Software). For the chi-squared and *t*-tests, a small *p*-value (less than 0.05, say) suggests that the data discredit the associated null hypothesis.

RESULTS

Coupons of 316L SS with a 2B finish, when examined in an as-received (unpolished), state using a metallurgical microscope, exhibited a surface oxide film that was discontinuous (Fig. 2(a)). The same surface, when viewed at higher magnification by confocal scanning laser microscopy (CSLM) with reflected white light, exhibited a surface oxide film delineated by grains which appeared as white or lighter shades of gray and the region between grains (grain boundaries) which appeared as black or darker shades of gray (Fig. 2(b)). Grains exhibited a mean surface area of 92 μm^2. Coupons prepared from
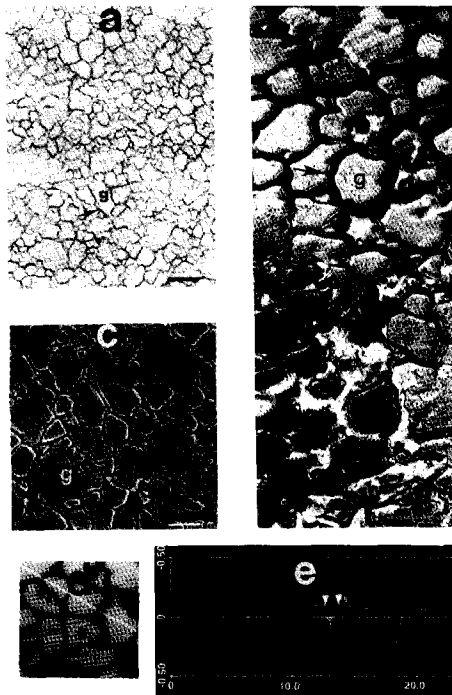

Fig. 2. Surface of as-received 316L stainless steel coupon with 2B finish (unpolished) as imaged by (a) metallurgical microscopy, (b) reflected white light confocal scanning laser microscopy, (c) scanning electron microscopy and (d) atomic force microscopy. Grains (g) and grain boundaries (arrow) in the oxide film can be resolved by each method. A topographic map of the surface obtained by atomic force microscopy is presented in (e). The white line in (d) defines path of the probe from which the topographic map was obtained. The depression in the film at the grain boundaries was determined from the vertical distance between the arrows positioned at the top of a grain and bottom of an adjacent grain boundary. The width of the grain boundary was determined by the distance between the edges of adjacent grains. Bar = 20 μm in (a) and 10 μm in (b),(c) and (d). Axes in (e) are in μm.

G. G. Geesey *et al.*

other lots of rolled 316L SS sheets with a 2B finish also displayed these surface features. These same features were preserved even after coupon cleaning, repassivation and exposure to flowing aqueous medium for 7 days. These features disappeared, however, after electropolishing.

Grains and grain boundaries in the oxide film were also observed on as-received coupons when viewed by scanning electron microscopy (Fig. 2(c)). Atomic force microscopy (AFM) of a cleaned, passivated coupon exposed to flowing aqueous medium revealed the oxide film grain boundaries (dark areas) as depressions between the grains (light areas) (Fig. 2(d)). The mean width and depth of the grain boundaries were 1.6 and 0.6 μm, respectively, based on AFM scans collected across 24 grain boundaries (Fig. 2(e)).

To determine whether there was a relationship between the grain structure of the surface oxide film elucidated by the microscopic methods described above and the grain structure of the bulk alloy, as-received coupons were polished and etched and then examined under a metallurgical microscope. Coupons prepared in this manner exhibited a typical austenite grain structure and no evidence of annealing twins (Fig. 3). The mean area of a grain was 211 μm^2 ($n = 134$). The area of grains varied from 15–1783 μm^2. There was no evidence of carbide precipitation at the grain boundaries, indicating that the metal had not been sensitized. Although the area of grains in the surface oxide film was not significantly different from the area of grains in the bulk alloy due to the wide range of areas observed, the mean area of oxide grains was half that of the grains in the bulk alloy. Thus, the grains of oxide film do not appear to conform to the underlying bulk grain structures.
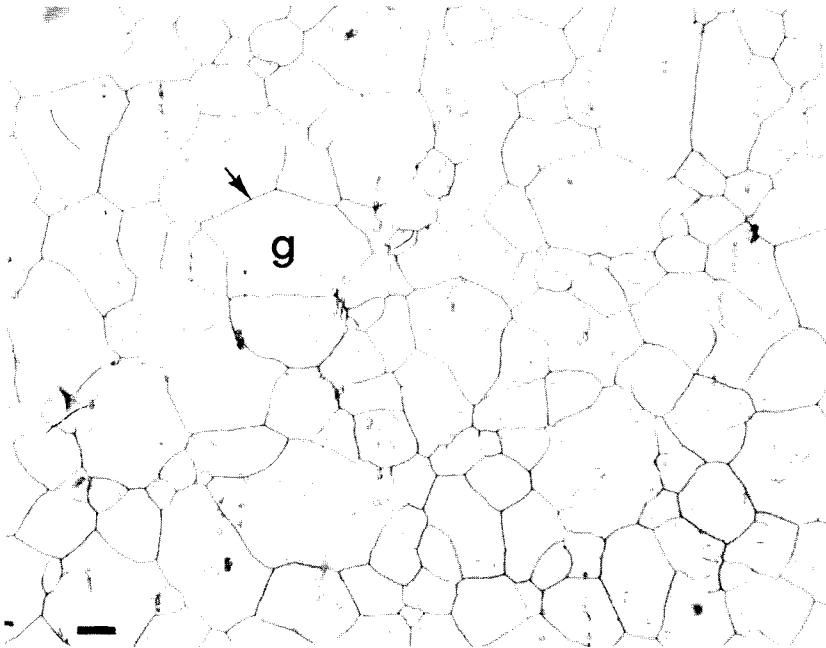

Fig. 3.   Surface of as-received 316L SS coupon with 2B finish after polishing and etching as imaged by metallurgical microscopy. g = grain, arrow = grain boundary. Bar = 10 μm.

Fig. 4.   Epifluorescent image of acridine orange-stained, surface-associated cells of *C. freundii* (light objects) superimposed on reflected white light image of surface features of oxide film on 316L SS obtained by confocal scanning laser microscopy after 16 day colonization period. Gray areas represent grains while darker areas which separate grains represent grain boundaries in oxide film. Bar = 10 μm.

Coupons recovered from the part of the reactor inoculated with a pure culture of *C. freundii* exhibited a non-random pattern of bacterial colonization. Images obtained by epi-illumination of acridine orange stained cells, when superimposed on reflected white light images of the coupon surface using a confocal scanning laser microscope, revealed a strong partitioning of these bacteria with oxide film grain boundaries as demonstrated after a 16 day exposure period shown in Fig. 4. The density of *C. freundii* on the coupon was 5.5×10^7 cells cm^{-2} based on direct microscopic counts of DAPI-stained bacteria on undisturbed surfaces (Table 5).

Although bacterial densities increased on the coupon surface with time, the partitioning of cells with grain boundaries was maintained over a 2–4 week period (Fig. 5). Eventually, the bacterial densities on the coupon became so high that the boundaries between grains in the oxide film were obscured.

Evaluation of 63 randomly selected coupon areas from four independent experiments indicated that oxide film grain boundaries contributed an average of 32.4% (range of

Table 5. Density of bacteria (cells/cm^2) in undisturbed biofilm on 316L
stainless steel coupon exposed to EPRI medium in anaerobic flow reactor

Conditions	Duration (days)	*C. freundii*	*D. gigas*
D. gigas only	9		
Exp. 1			$4.2 \pm 2.8 \times 10^3$
Exp. 2			$6.9 \pm 0.9 \times 10^2$
Co-culture	9		
Exp. 1			$4.3 \pm 2.6 \times 10^4$
Exp. 2			$1.1 \pm 0.1 \times 10^4$
Co-culture	14		
Exp. 1		$5.1 \pm 1.2 \times 10^7$	$4.6 \pm 0.2 \times 10^3$
Exp. 2		$4.9 \pm 0.2 \times 10^7$	$1.1 \pm 0.1 \times 10^4$
C. freundii only	14	$5.5 \pm 1.7 \times 10^7$	

11–47%) of the total surface area. An average of 76.6% (range of 61–90%) of the total
number of bacteria present on the coupon surface over the 2–4 week exposure period
were located within these grain boundaries (Fig. 5). The low percentage contribution of
grain boundaries to the coupon surface area and large standard deviation for the
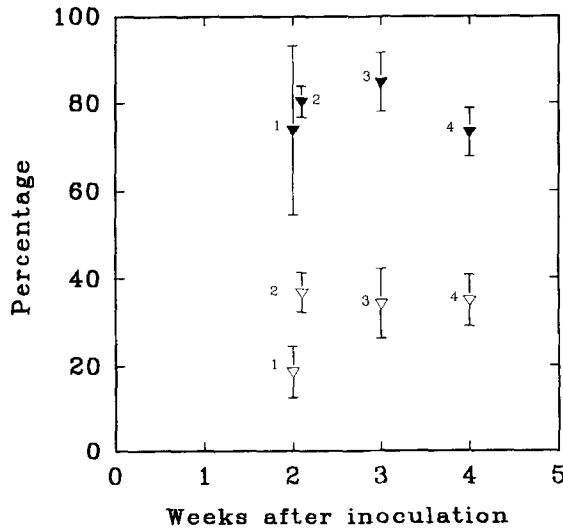percentage of total surface-associated bacteria present within the grain boundaries in

Fig. 5. Percentage of the total oxide film surface area (grains + grain boundaries) contributed by
oxide film grain boundaries ($\triangledown$) and percentage of the total surface-associated *C. freundii* bacterial
cells that are located at grain boundaries ($\blacktriangledown$) on coupons at different times after inoculation of
bacteria to the reactor. Numerals adjacent to data points identify corresponding data sets. The
number of images analysed to obtain each data point was $n = 9$, $n = 19$, $n = 19$ and $n = 16$ for data
sets 1, 2, 3 and 4, respectively. Bar represents ± 1 standard deviation.

Experiment 1 were due to initial problems with software programming and collection of an insufficient number of images, respectively.

If the bacteria were randomly distributed over the surface, the fraction of the total population located within the oxide film grain boundaries should not be significantly different from the fraction of the total area contributed by the grain boundaries. The difference was significant ($p < 0.0001$). The chi-square test statistic was $C = 11,626$ ($p = 0.0000$) for data from the four experiments presented in Fig. 5. These results indicate that cells of *C. freundii* have a strong preference for colonizing grain boundaries over grains in the surface oxide film on 316L SS.

Coupons from anaerobically-operated reactors that were inoculated with either pure cultures of *D. gigas* or co-cultures of *D. gigas* and *C. freundii* contained densities of *D. gigas* that were too low, even after 4 weeks incubation, to determine whether the SRB, like *C. freundii*, exhibited a preference for the grain boundaries in the oxide film. Nevertheless, *D. gigas* did attach to and colonize coupons in anaerobically operated reactors. The number of cells of *D. gigas* that colonized the coupons over a 9-day period was significantly higher when introduced as a co-culture with *C. freundii* than when grown as a pure culture based on direct microscopic enumeration of undisturbed biofilms using DAPI staining (Table 5). In contrast, coupon-associated cell densities of *C. freundii* were not significantly different when the coupon was colonized for 14 days by a pure culture of this bacterium or co-colonized by the SRB (Table 5).

EDX/SEM analysis of the stainless steel coupon surface before introduction to the reactor revealed Cr, Ni and Fe elemental abundances that were similar to the bulk elemental abundances supplied by the manufacturer for the as-received coupons (Table 6). No significant differences were detected in elemental abundance collected within areas defined as grains and grain boundaries in the surface oxide film (data not shown). This is consistent

Table 6. Abundance of various elements as a percentage of all elements detected in unpolished, passivated 316L stainless steel coupons used for reactor studies†

Element	Oxide film grain‡	Oxide film grain boundary‡	bulk§	Nominal bulk as received¶
Cr	10.7	10.4	18.1	17.4
Ni	10.2	11.2	10.1	11.2
Fe	63.9	53.9	69.5	67.1
C	7.2	12.0	<2.0	0.022
O	5.3	8.5	<2.0	nd
Si	2.7	3.0	<2.0	0.07
Mo	nd	nd	2.3	2.17
Other	nd	nd	<2.0	2.10
Total	100	99.0	100	100

†Each number is the mean of 3 EDX or small spot AES analyses.
‡Elemental composition of near-surface region of oxide film at grains and grain boundaries as determined by AES analysis.
§Elemental composition of bulk as determined by EDX analysis.
¶Nominal elemental composition provided by manufacturer.
nd, no data

with the fact that EDX surveys the top 800 nm of the coupon, penetrating into the bulk well beneath the surface oxide film which has been reported to be of the order of 2–5 nm in thickness.

Small spot (250 nm dia.) AES analysis of the same coupon revealed elemental abundances at grains and grain boundaries in the oxide film immediately below the heavily carbon contaminated region (approximately 6 nm below the surface) that, for Cr and Fe, are lower than those reported for the bulk material (Table 6). There was much less variation in abundance of Ni between this near-surface region and bulk metal than there was for Cr and Fe. The abundance of Cr and Ni at the near-surface did not differ significantly between areas defined by grains and grain boundaries in the oxide film. Fe appeared more depleted at the near-surface of the oxide film within grain boundaries than within grains, although these differences may be due to the differences contributed by the non-alloy elements, carbon, oxygen and silicon (Table 6).

If one takes into account the effect that the presence of non-alloy elements (C,O and Si) had on the abundance of the alloying elements at the grain boundaries in the oxide film, Cr would be depleted 2.7% and Fe and Ni would be enriched 3.3 and 2.7% relative to their bulk abundances in the as-received material. At the grains, Cr, Fe and Ni would be enriched 1.6, 9.7 and 1.6%, respectively, relative to their bulk abundances. In order to cancel the effects of non-alloying elements on the relative abundance of the alloying elements in the surface film during coupon exposure to colonizing micro-organisms, the latter were expressed as a ratio based on Ni abundance. Nickel was selected as the normalizing element because it exhibited the least variation of the alloying elements evaluated under the conditions used in these studies.

AES analysis of the near-surface region of the coupon was performed in the same manner as above after exposure of the coupons for increasing periods of time to flowing, sterile, anaerobic culture medium in reactors that were either uninoculated (sterile control) or inoculated with a co-culture of *C. freundii* and *D. gigas*. The abundance of Cr relative to Ni decreased at grain boundaries but not at grains in the surface film during a 4 week period of exposure to and colonization by a coculture of these bacteria (Fig. 6). In the first 2 weeks of exposure, when the surface film grain boundaries were largely uncolonized by bacteria, no significant difference in the Cr/Ni ratio was observed between grains and grain boundaries. After 3 weeks, however, the Cr/Ni ratios at grains and grain boundaries were significantly different ($p < 0.0001$). During the 3 week period following inoculation, the bacteria had time to preferentially colonize a larger portion of the grain boundaries than at previous observation periods. The Cr/Ni ratios at surface film grains and grain boundaries continued to diverge between 3 and 4 weeks, primarily as a result of further Cr depletion relative to Ni at the grain boundaries. No significant difference in the Cr/Ni ratios was observed at grains and grain boundaries in the surface film of coupons exposed to sterile aqueous medium for at least 4 weeks (Fig. 6). Similar trends were observed in the relative abundance of Fe to Ni (Fig. 7).

The Cr/Ni ratios at grains and grain boundaries on the surface oxide film of coupons exposed to either sterile aqueous medium, monocultures of *C. freundii*, or cocultures of *C. freundii* and *D. gigas* were compared after 2 weeks. The Cr/Ni ratio at grains decreased by approximately 20% on coupons exposed to either a monoculture of *C. freundii* or a coculture of *C. freundii* and *D. gigas* relative to that of the sterile control (Table 7). The Cr/Ni ratios at grain boundaries on the surface film decreased by 35 and 32% following exposure to a monoculture of *C. freundii* and a coculture of the two types of bacteria,
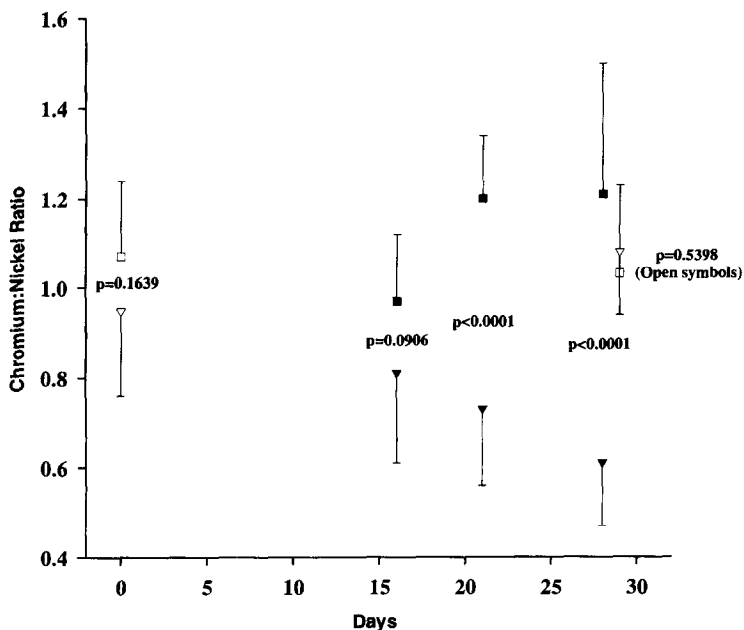
Fig. 6. Ratios of the atomic percent abundance of chromium to nickel in near surface regions of the oxide film at grains (squares) and grain boundaries (triangles) of 316L SS coupons after exposure to sterile EPRI medium (open symbols) or to *C. freundii* + *D. gigas* (solid symbols) for various periods of time. Data was obtained by small-spot AES after a 60 s sputter time. Each data point represents the mean value of elemental spectra collected from nine different areas on the coupon. Bar represents ± 1 standard deviation. (Only deviation in one direction is presented to minimize overlap of bars from different data points in this and subsequent figures.) *p*-values in this and subsequent figures represent the probability that the mean values of data obtained at grains and grain boundaries at different sampling times are not significantly different.

respectively. These results suggest that the presence of bacteria promotes Cr depletion relative to Ni at both types of surface features, that the Cr depletion was more pronounced at grain boundaries than at grains and that the depletion is promoted primarily by *C. freundii* since no additional decrease in the ratio was observed in the presence of *D. gigas*, at least during the first 2 weeks of exposure. Based on the results of this 2-week study and the 4-week study described above, it appears that the bacteria cause significant changes in Cr/Ni ratios in the near-surface layer of the oxide film in the 2–3 week period following initiation of coupon colonization.

D. gigas did appear to have an influence on Fe abundance relative to Ni at grain boundaries in the surface film during the first 2 weeks of exposure of the coupons to the SRB. While the Fe/Ni ratio at grains was similar in the presence of *C. freundii* with or without *D. gigas*, the ratio at grain boundaries was lower in the presence of the coculture (4.0) than with *C. freundii* alone (4.4) (Table 7). The ratio in the presence of the SRB was 63% of the control while the ratio in the absence of the SRB was 70% of the control. Whereas the differences in the ratios at grains and grain boundaries were not significant in the sterile control or in the presence of *C. freundii* alone, the difference was significant when
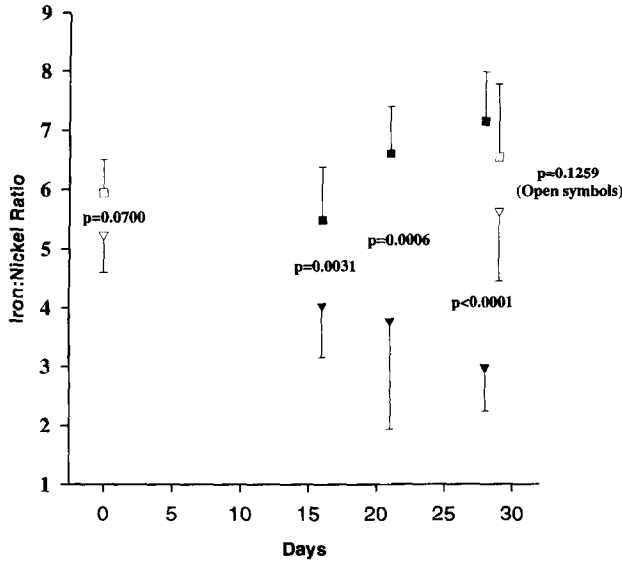
Fig. 7. Ratios of the atomic percent abundance of iron to nickel in near-surface regions of the oxide film at grains (squares) and grain boundaries (triangles) of 316L SS coupons after exposure to sterile EPRI medium (open symbols) or to *C. freundii* + *D. gigas* (solid symbols) for various periods of time as described in Fig. 6.

D. gigas was present (Table 7). Thus, over a 2 week period, Fe depletion relative to Ni is significantly enhanced at grain boundaries but not at grains by the presence of the SRB.

The presence of bacteria appeared to influence the levels of sulfur that accumulated at the surface features of the surface oxide film on the coupons. While coupons exposed to sterile, sulfur-containing culture medium contained significantly higher concentrations of sulfur at grain boundaries than at grains, coupons exposed to either a monoculture of *C. freundii* or to cocultures of *C. freundii* and *D. gigas* had significantly higher levels of sulfur at both grains and grain boundaries than coupons exposed to sterile, sulfur-containing culture medium (Fig. 8). Coupons exposed to the cocultures had significantly higher levels of sulfur near the surface of the oxide film at grain boundaries than coupons exposed to

Table 7. Relative abundance of alloy elements near the surface of the oxide film on 316L stainless steel after 2 weeks exposure to EPRI medium in flow reactor with and without bacteria†

Ratio	Bulk	Control		*C. freundii* only		*C. freundii* + *D. gigas* (from Figs 6 and 7)	
		Grain	Grain B	Grain	Grain B	Grain	Grain B
Cr/Ni	1.8	1.2(0.25)	1.2	0.98 (0.01)	0.78	0.97 (0.09)	0.82
Fe/Ni	7.0	7.0(0.15)	6.3	5.4 (0.11)	4.4	5.5 (0.003)	4.0

†Ratio of mean values; each mean is based on three observations.

Numbers in parentheses represent *p*-values derived from differences in ratios obtained from grains and grain boundaries (Grain B) in oxide film.
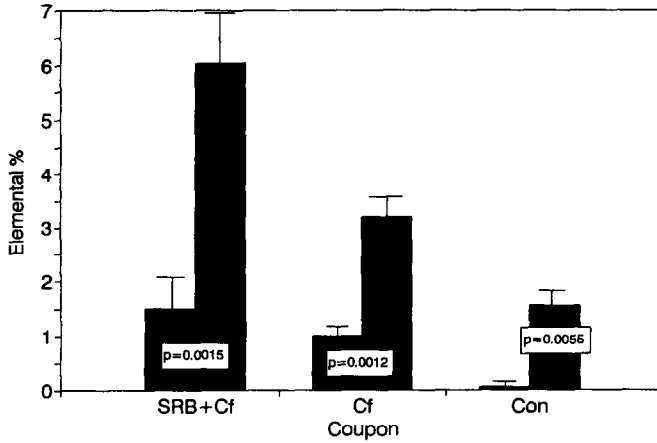
Fig. 8. Atomic percent abundance of sulfur with respect to all other elements detected in near-surface regions of the oxide film at grains (solid bar) and grain boundaries (hatched bar) of 316L SS coupons exposed to sterile medium (Con) or to an inoculum of *C. freundii* with (Cf + SRB) or without (Cf) an inoculum of *D. gigas* based on small-spot AES after 60 s sputter time to penetrate the carbon contaminated surface layer.

monocultures of *C. freundii*. These results indicate that the SRB contributed to sulfur accumulation at these locations. The SRB did not appear to have a significant influence on sulfur accumulation near the surface of the oxide film on the grains, at least during the first 2 weeks of exposure (Fig. 8). The higher levels of sulfur at the grain boundaries than at grains may simply reflect differences in the efficiency of removal of biofilm products from
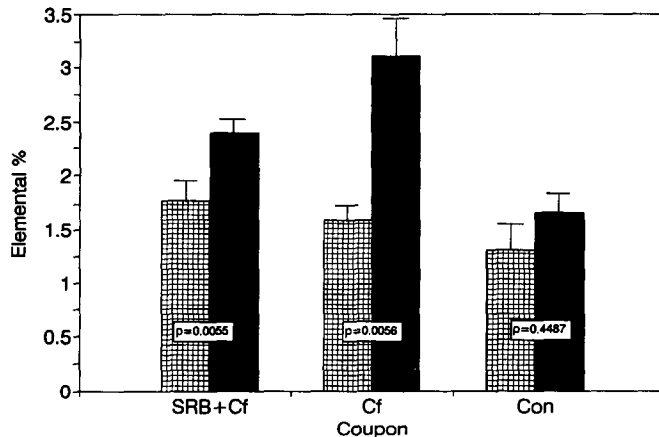

Fig. 9. Atomic percent abundance of nitrogen with respect to all other elements detected in near-surface regions of the oxide film at grains (solid bar) and grain boundaries (hatched bar) of 316L SS coupons exposed to sterile medium (Con) or to an inoculum of *C. freundii* with (Cf + SRB) or without (Cf) an inoculum of *D. gigas* based on small-spot AES after 60 s sputter time to penetrate the carbon contaminated surface layer.

these surface features before AES analysis in the case of those coupons exposed to bacteria. That this trend exists in the sterile control as well, suggests that dissolved sulfur compounds in the aqueous medium have a greater tendency to accumulate in the physical depressions of the grain boundaries than on the grains of the surface oxide film.

In contrast, nitrogen, presumably derived from medium components, does not appear to exhibit significant preference for grain boundaries in the abiotic control coupons, and while there is a significant preference for nitrogen at grain boundaries over grains in the surface film of coupons exposed to and colonized by bacteria, the SRB has no discernable impact on this preference (Fig. 9). Thus, while sulfur-containing compounds derived from either the bulk solution or the biofilm bacteria preferentially accumulate at grain boundaries in the absence or presence of bacteria, but particularly in the presence of SRB, nitrogen-containing compounds show little preference for these metallurgical features in the absence of bacteria.

DISCUSSION

Unpolished, as-received, 316L SS coupons with a 2B finish as well as coupons which have been subsequently cleaned, repassivated and exposed to flowing aqueous medium (but not polished) exhibit a surface oxide film containing grains and grain boundaries as the primary surface features. While the grains of the oxide film do not appear to correspond to the underlying grain structure of the bulk alloy based on mean surface area determinations, there was significant overlap in the range of areas of these features.

The results from this study confirm earlier reports that micro-organisms accumulate at discontinuities on submerged metal surfaces.[11,27] A strong partitioning of cells of *C. freundii* at surface oxide film grain boundaries in an anaerobic, continuous-flow reactor was verified by a combination of CSLM, image and statistical analysis. Walsh *et al.*[11] showed that following random attachment, proliferation and/or aggregation of bacteria at any given location is determined by proximity to metallurgical features such as inclusions. The present CSLM images reveal primarily single cells oriented along grain boundaries in the surface oxide film prior to proliferation at these locations, suggesting that initial colonization is non-random and highly selective for this surface feature over grain areas in the oxide film. Selective accumulation of cells at grain boundaries became evident within 2 weeks and continued over the 4-week observation period. Thus, this trend extends for some time after initial colonization, leading to long-term patchiness in surface coverage by the surface-associated bacteria and offering ample opportunity for the initiation of localized corrosion that might evolve from such biological heterogeneity. After 1 month, bacterial colonization and growth on the coupon surface obscured the boundaries of the grains in the oxide film, compromising characterization of this phenomenon over longer time periods.

The extent to which bacteria depend on topographical or chemical cues at surface oxide film grain boundaries is of general interest. AFM demonstrated that a grain boundary occurred as a cavity or depression in the oxide film. Surface associated bacteria are often found concentrated in cavities on particle surfaces in nature, so it is not surprising that this is where they congregate at metal surfaces.[28] Like grain boundaries in the bulk alloy, those in the surface oxide film may represent a region of high surface energy which may promote attachment and colonization of some bacteria. Polishing the surface of the alloy, a common practice before placing the material in service, is likely to interfere with the selective colonization process due to the fact that it destroys these surface features. Additional work

is planned, however, to further investigate the relative importance of physical and chemical cues for bacterial colonization of this alloy.

Breummer[12] provided EDX evidence that a bulk Cr content of 13.5% is necessary for corrosion resistance in 304 SS. Chromium depletion of grains in the bulk alloy at weldments and heat affected zones due to welding leads to preferential anodic dissolution in 304 SS.[13] The extent to which Cr content in different regions of the protective oxide film influences corrosion resistance is less clear.

The elemental abundance of passive films of stainless steels formed under a variety of conditions has been described previously using AES. Ramasubramanian et al.[30] reported that air-formed oxide films on as-received 316L SS were Cr-enriched and Fe-depleted at the steel–oxide interface but Cr-depleted and Fe-enriched in the surface layers of the film relative to elemental abundances in the bulk steel. Inclusion of a cathodic reduction step prevented the reversal at the surface layers, however. Olefjord and Fischmeister[31] found that when the oxide film was formed in a dry oxygen environment, depletion of chromium occurred in the outermost layer of the film, but there was slight enrichment of Cr at the metal/oxide interface. Prolonged exposure to an aqueous environment led, however, to Cr enrichment in the outermost portion of the film.[31] Thus, the abundance of the alloying elements in the surface oxide film varies depending upon the conditions to which the material is exposed. The present studies indicate that the development of a microbial biofilm on the surface of a 316L SS coupon leads to both Cr and Fe depletion relative to Ni at a subsurface location in the oxide film.

While other studies have shown attack at a grain boundary in the bulk metal adjacent to accumulations of bacterial cells[11], this is the first study to our knowledge that relates statistically significant chemical differences at surface features of the oxide film on unpolished 316L SS to the presence of bacteria at these features.

Chromium, already depleted relative to the bulk material in a region approximately 6 nm below the surface of the carbon-contaminated oxide film at grain boundary locations before exposure to micro-organisms, becomes significantly more depleted relative to Ni at grain boundaries compared to grains during increased periods of time of coupon exposure to and colonization by cells of C. freundii. No significant depletion of Cr relative to Ni occurred in this near-surface region at grain boundary locations in the oxide film on coupons exposed to sterile, yet otherwise identical, conditions during the period of study. This indicates that the near-surface depletion of Cr with respect to Ni at these sites in the presence of the bacteria was linked to biofilm processes on the surface of the oxide film. Furthermore, these biological effects on oxide film chemistry did not require a thick, confluent biofilm but rather occurred as a result of a heterogeneous distribution of bacteria with only partial coverage over the surface.

The presence of carbonaceous material derived from the organic compounds in the aqueous phase or the adherent bacteria at the surface of the chromium oxyhydroxide film precluded elucidation of the abundance of alloy elements in regions of the surface film where these contaminating materials were concentrated. Carbon contamination is often encountered on surfaces by surface-sensitive spectroscopic techniques.[29] Extensive sputtering of surfaces that contain levels of carbon contamination such as those encountered under the conditions used in the present studies is often required before features of the oxide film are resolved. Cieslak and Duquette[29] arbitrarily sputtered their surfaces until 75% of the carbon contamination was removed. The report of abundances of alloying elements after sputtering through approximately 90% of this carbon permitted

identification of a near-surface region of the oxide film where a biological effect on oxide film chemistry occurred. That the surface of the oxide film on coupons recovered from sterile controls also exhibited extensive carbon contamination indicates that at least some of this carbon is derived from organic compounds adsorbed from the bulk aqueous phase.

Chromium, presumably in an ionized state, often accumulates in areas where localized corrosion has already occurred. Stoecker and Pope[5] examined a failed tank constructed of 304 stainless steel and found that Cr increased from a low of 19.10% in the matrix metal to a high of 37.10% in cracks while Ni dropped from a high of 10.61% in the metal matrix to a low of 1.81% in the cracks when examined by EDX. The cracks, which eminated from pits that were overlaid by surface deposits, seemed to be extensions of grain boundaries. Likewise, Cubicciotti and Licina[13] showed that pitted areas of various alloys, including 316 SS, had a much enriched Cr content, less Ni and a thinner oxide film.

Reconciliation of present results with those reported by Stoecker and Pope[5] and Cubicciotti and Licina[13] requires that another region of the surface film not sampled by the current method exhibits an enrichment of Cr that, when combined with other regions sampled by EDX, yields higher levels of this element at corroded areas than at noncorroded areas of a coupon. It cannot be determined at this time whether there is a Cr-enriched region above or below the region in the surface film which was sampled by AES because of constraints associated with this method. In addition, the elemental abundance presented in these other studies were obtained from surfaces at advanced stages of corrosion that contained an accumulation of corrosion product on the surface. No morphological evidence of corrosion or corrosion deposit was observed on the surface of any of the coupons sampled in the present study.

The trend of increasing Cr depletion relative to Ni at grain boundaries in near surface regions of the oxide film during early stages of bacterial colonization and biofilm development reported here may weaken the oxide film, allowing halides such as Cl$^-$ greater access to the underlying bulk alloy at these locations.[29] This would facilitate pitting attack in areas where micro-organisms have congregated. That partitioning of the bacteria at grain boundaries in the surface film is maintained for periods of at least 4 weeks supports the idea that surface heterogeneities propagated by bacterial colonization can be stable over time.

Although the SRB density on the coupon surfaces was relatively sparse compared to the density of *C. freundii*, it appeared to be sufficient to cause a significant decrease in Fe relative to Ni as well as a significant increase in sulfur accumulation in the near-surface regions of the oxide film at grain boundaries when compared to the abundance of these elements at comparable surface features on coupons exposed only to *C. freundii* over a 2-week exposure period. Comparable densities of surface-associated SRB have been reported in cases of corrosion of mild steel pipelines.[32] Recently Jain[33] showed that *C. freundii* promoted the growth of *D. gigas* in semisolid Postgate's B Medium. It was also observed that *C. freundii* promoted the growth of *D. gigas* in preliminary studies in anaerobic EPRI medium (data not shown). Thus, selective colonization of grain boundaries in the oxide film of 316L SS by *C. freundii* may lead not only to chromium depletion but also to iron depletion relative to Ni and to sulfur accumulation in near-surface regions of the oxide film by promoting colonization of *D. gigas* at these sites. To date, it has not been possible to obtain high enough densities of the SRB on the coupon in the presence or absence of *C. freundii* to permit application of the statistical approach used here for *C. freundii*. Culture conditions are presently modified to enhance further *D. gigas* colonization of this alloy for this purpose.

Pitting attack of stainless steel alloys in the presence of sulfate reducing bacteria occurs at inclusions which contain sulfur.[18,34] The ability of SRB to produce acidic as well as sulfidic end-products is cited as the main factor in the initiation of corrosion in these alloys. Sulfide produced by the surface-associated *D. gigas* may mobilize iron and promote formation of an iron sulfide deposit that is cathodic to steel.[35] Some sulfur did accumulate in the near-surface regions of the oxide film at grain boundaries on coupons exposed to monocultures of *C. freundii* as well as sterile culture medium. Since it was not possible to distinguish between the various forms of sulfur that accumulated under these different conditions, it is not yet possible to attribute the observed iron depletion at grain boundaries to specific metabolic products. However, future studies are planned to resolve this issue.

Deshmukh *et al.*[18] observed greater numbers of pits and corrosion spots on 304 SS in the presence of a mixed culture of *Comamonas testosteronii* and *Desulfovibrio vulgaris* than in the presence of either species alone. Corrosion attack seemed to be of an intergranular nature. In contrast to the results of Deshmukh *et al.*,[18] Ringas and Robinson[34] reported no notable difference in the corrosion rate of various alloys, including 316L SS, in the presence of monocultures and mixed cultures of SRB. The initiation of pitting corrosion that was observed at intergranular regions in the presence of SRB was not observed in sterile controls. Present results support the observations of Deshmukh *et al.*[18] that, compared to monoculture biofilms, mixed culture biofilms accelerate the establishment of conditions that have been shown to promote intergranular attack of stainless steel, as well as the results of Ringas and Robinson[34] that these conditions do not develop in the absence of bacteria.

CONCLUSIONS

1. Unpolished coupons of 316L stainless steel with a 2B finish exhibit grains and grain boundaries in the oxide film when viewed by a variety of microscopic techniques.

2. The facultatively anaerobic bacterium, *C. freundii*, selectively colonized depressions at the grain boundaries in the surface film of coupons exposed to flowing aqueous medium over a 1 month period.

3. Selective colonization by *C. freundii* resulted in significant depletion of chromium relative to Ni at grain boundaries compared to grains in near-surface regions of the surface film.

4. Significant depletion of iron relative to Ni was observed in near-surface regions of the oxide film at grain boundaries when colonized by a co-culture of *C. freundii* and *D. gigas* but not in coupons maintained under sterile conditions or in the presence of *C. freundii* alone.

5. These microbiologically-induced chemical changes in near-surface regions of the oxide film on unpolished 316L stainless steel which occur during early stages of surface colonization and biofilm development may be critical steps that lead to subsequent localized attack when the alloy is commissioned for service in this state.

REFERENCES

1. G. Kobrin, *Mat. Perform.* **15**(7), 38 (1976).
2. R. E. Tatnall, *Mat. Perform.* **20**(8), 41 (1981a).
3. R. E. Tatnall, *Mat. Perform.* **20**(9), 32 (1981b).
4. D. H. Pope, D. J. Duquette, A. H. Johannes and P. C. Wayner, *Mat. Perform.* **23**(4), 14 (1984).
5. J. G. Stoecker and D. H. Pope, *Mat. Perform.* **25**(6), 51 (1986).
6. V. Scotto, G. Alabiso and G. Marcenaro, *Bioelectrochem. Bioenerg.* **16**, 347 (1986).
7. R. E. Tatnall, *Proc. of the National Meeting of the Society of Corrosion Engineers*, Paper No.95, New Orleans, (1984).
8. R. J. Soracco, D. H. Pope, J. M. Eggers, and T. N. Effinger, *Proc. of the National Meeting of the Society of Corrosion Engineers*, Paper No. 83, St. Louis (1988).
9. C. R. Das and K. G. Mishra, *Biologically Induced Corrosion*, p. 114. National Association of Corrosion Engineers, Houston (1985).
10. S. Borenstein, *Mat. Perform.* **30**(1), 52 (1991).
11. D. Walsh, D. Pope, M. Danford and T. Huff, *J. Min. Met. Mat. Soc.* **45**(9), 22 (1993).
12. S. M. Bruemmer, *Mat. Sci. Forum* **46**, 309 (1989).
13. D. Cubicciotti and G. J. Licina, *Mat. Perform.* **29**(1), 72 (1990).
14. B. Little, J. Jacobus and L. Janus, *Estuaries* **12**, 138 (1989).
15. J.-R. Chen, S.-D. Chyou, S.-I. Lew, C.-J. Huang, C.-S. Fang and W.-S. Tse, *Appl. Surf. Sci.* **33/34**, 212 (1988).
16. J. W. Costerton and G. G. Geesey, *Biologically Induced Corrosion*, p. 223. National Association of Corrosion Engineers, Houston (1985).
17. R. F. Mueller, W. G. Characklis, W. L. Jones, and J. T. Sears, *Biotechnol. Bioengineer.* **39**, 1161 (1992).
18. M. B. Deshmukh, I. Akhtar, R. B. Srivastava and A. A. Karande, *Biofouling* **6**, 13 (1992).
19. P. J. Bremer, G. G. Geesey and B. Drake, *Curr. Microbiol.* **24**, 223 (1992).
20. R. A. Lula, *Stainless Steel*, p.93. Am. Soc. Metals, Metals Park, OH (1986).
21. ASTM Standard Practice for Cleaning and Descaling Stainless Steel Parts, Equipment, and Systems, A-380-78. Code B, American Society for Testing and Materials, Philadelphia, Pennsylvania (1987).
22. *ASM Metals Handbook*, 9th Ed., Vol. 9, p 282 (1985).
23. G. Cohen-Bazire, W. R. Sistrom and R. Y. Stanier, *J. Cell. Comp. Physiol.* **49**, 25 (1957).
24. N. S. Battersby, D. J. Stewart and A. P. Sharma, *J. Appl. Bacteriol.* **58**, 425 (1985).
25. C. A. Zapffe, *Properties and Selection of Metals Handbook*, Vol. 1, p. 408. American Society for Metals, Metals Park, OH (1961).
26. L. E. Davis, N. C. Macdonald, P. W. Palmberg, C. E. Raich and R. E. Weber, *1976 Handbook of Auger Electron Spectroscopy*, p. 249. Physical Electronics Industries, Inc., Eden Prairie, MN (1976).
27. G. G. Geesey, W. G. Characklis and J. W. Costerton, *ASM News* **58**(10), 546 (1992).
28. G. G. Geesey and J. W. Costerton, *Can. J. Microbiol.* **25**, 1058 (1979).
29. W. R. Cieslak and D. J. Duquette, *Corrosion* **40**(10), 545 (1984).
30. N. Ramasubramanian, N. Preocanin, and R. D. Davidson, *J. electrochem. Soc.* **132**(4), 793 (1985).
31. J. Olefjord and H. Fischmeister, *Corros. Sci.* **15**, 697 (1975).
32. J. W. Costerton and J. Boivin, *Biological Fouling of Industrial Water Systems: A Problem Solving Approach*, p. 56. Water Micro Associates, San Diego, CA (1987).
33. D. K. Jain, *J. Microbiol. Methods* **22**, 27 (1995).
34. C. Ringas and F. P. A. Robinson, *Corrosion* **44**, 671 (1988).
35. G. Wranglon, *Corros. Sci.* **9**, 585 (1969).

APPENDIX

The images were processed independently in a series of steps. First, MARK located the x,y positions of bacteria for a particular field by an automated estimation of each bacterial location in relation to the centroid of its perimeter. Each centroid was denoted by a red 'X', with its x,y position saved in a data file. The bacterial image was cleared from the screen.

Then, the reflected white light image of the same field was processed. Surface features of the coupon were visually distinct when viewed microscopically using reflected white light. Two contrasting surface features can be seen in each field of view; one which appears as white or lighter shades of grey which shall be referred to as grains of the surface oxide film and another which appears black or in darker shades of grey which shall be referred to as grain boundaries between the grains of the oxide film. For each coupon examined, a digitized image of each field of view was captured for quantification with MARK.

A stored image consists of a set of ordered triples (X,Y, pixel shade = 1). For each image of a coupon surface, the histogram of the pixel shades was bimodal. It is possible, via a shade cutpoint routine in MARK, to count the number of black grain boundary pixels on the surface of a coupon. This approach permitted determination of the dimensions of these surface features.

Because the corners of the images were out-of-focus, statistical analysis was applied to the interesting regions called the area of interest (AOI). Each AOI was chosen by drawing with the computer mouse a closed polygon over the image of the coupon surface. The boundary of the AOI appeared on the image as a yellow line. The number of black pixels corresponding to the area contributed by oxide film grain boundaries within the AOI was then calculated. The number was converted into the percentage of black pixels in the AOI compared to the total number of pixels within that same area and then recorded as the percentage grain boundaries (P_i). The x,y positions from the matching bacterial locations file were overlaid as red Xs on the surface image file. At this point, the Xs lying outside the area of interest were deleted. Then, the color of the Xs was manually changed, depending on the position of the X relative to a grain boundary. If an X was on or touching a grain boundary, it remained its original red color. If an X was on a grain, its color was changed to yellow. Once all the Xs on the area of interest were evaluated, the x,y position, corresponding pixel value and numerical color number (red $= 0$, yellow $= 1$,) were saved on a separate file. From these data, the percentage of bacteria on film grain boundaries (Q_i) compared to the percentage of area containing grain boundaries (P_i) could be estimated for each image (i). These data were then subjected to statistical analysis.